A00-39779

AIAA Paper 2000-4135

# DYNAMICS AND CONTROL OF RELATIVE MOTION IN AN UNSTABLE ORBIT*

D.J. Scheeres† and N.X. Vinh‡
Department of Aerospace Engineering
The University of Michigan
Ann Arbor, MI 48109-2140

## Abstract

We study the relative dynamics and control of two spacecraft orbiting in close proximity in an unstable halo orbit. The understanding of a pair of such spacecraft is immediately extendable to the understanding of a constellation of such spacecraft. This is an issue of current interest given plans for space-based interferometric telescopes and the attractiveness of placing such systems in orbits about the $L_2$ libration point. The paper focuses on the specification of control laws to stabilize the relative motion, and analyzes the relative dynamics and fuel consumption of the spacecraft. A brief discussion of the relative orbit determination is also given.

## Introduction

This paper studies the stabilization of translational motion relative to an unstable periodic orbit in the Hill problem (which can be considered as a subset of the restricted 3-body problem). Results of this study will be relevant to the dynamics and control of a constellation of spacecraft in an unstable orbital environment such as found near the Earth-Sun libration points. It will also shed light onto the practical control and computation of a single spacecraft trajectory over long time spans.

We investigate the application of feedback control laws to stabilize the relative trajectory of the spacecraft in the sense of Lyapunov. Thus, the relative trajectory may still contain oscillatory motions, which in this context can be interpreted as stable motions in the center manifold of the periodic orbit – modified as a function of the applied control law. We show that an entire class of such control laws can be defined and their stability analyzed as a time periodic linear system. The fuel expenditure for such control laws is often quite small, but scales with the mean distance between the two spacecraft.

A fundamental problem with using center manifolds of an unstable orbit for relative motion is the difficulty of computing non-linear (or even linear) orbits that remain in the center manifold. The current state of the art (numerical and analytical) is given in Barden and Howell (1998) and Gómez et al. (1998). From these analyses we see that extremely precise computation (numerical or analytical) is required to maintain an orbit in the center manifold of an unstable halo orbit. Small deviations from the center manifold quickly cause the trajectory to diverge along the unstable manifold of the halo orbit.

In this paper we propose an approach which addresses the problem from a different direction, casting the problem as a trajectory control problem from the start. Using this methodology we change the focus of the computation from remaining in the center manifold to continually thrusting to remove components of motion in the hyperbolic manifolds. The basic control law to effect this is derived and applied to orbits about the unstable halo orbit. We conclude with some examples showing the control law at work in non-linear situations, and comment on the level of control acceleration needed and other practical issues of implementation.

## Model of Spacecraft Motion

For computing the non-linear motion of the spacecraft we use the Hill equations of motion, which are a simplified form of the 3-body problem applicable to the motion of a spacecraft near the Earth, accounting for the perturbation of the sun (Marchal,



†Assistant Professor of Aerospace Engineering; Senior Member AIAA; email: scheeres@umich.edu

‡Professor of Aerospace Engineering, Emeritus

p. 64). The three dimensional motion is governed by the equations:

$$\ddot{x} - 2\omega\dot{y} = -\frac{\mu}{r^3}x + 3\omega^2 x \quad (1)$$

$$\ddot{y} + 2\omega\dot{x} = -\frac{\mu}{r^3}y \quad (2)$$

$$\ddot{z} = -\frac{\mu}{r^3}z - \omega^2 z \quad (3)$$

where $\omega$ is the mean motion of the central, attracting body about the perturbing body (assuming circular motion), and $\mu$ is the gravitational attraction of the central body. In our situation we choose $\mu$ to be that of Earth and $\omega$ to correspond to an orbital period of one year. The $x$ axis lies along the line from the perturbing body to the central body and remains fixed in this rotating frame, the $y$ axis points along the direction of travel of the central body about the perturbing body, and the $z$ axis is normal to the ecliptic. These equations are non-integrable and exhibit a range of complex solutions, analogous to the restricted 3-body problem.

For our investigation we consider a periodic orbit solution of these equations, a halo orbit to be more specific, which is a fully 3-dimensional orbit centered about the libration points. Figures 1 – 3 show this particular halo orbit projected into the main coordinate planes. The initial conditions of this periodic orbit are chosen to be similar to the Genesis halo orbit during its main mission phase (Howell et al. 1997). The period of this orbit is 178.9 days. The orbit is unstable, with a single hyperbolic stable and unstable manifold with characteristic exponent $\sigma = 4.757 \times 10^{-7}$/s (a characteristic time of 24.3 days). The orbit also has two stable oscillation modes, one with period equal to the periodic orbit (as all periodic orbits have) and the other with period slightly greater than one orbital period.

We assume that the first spacecraft follows this periodic orbit. We do not discuss the navigation (i.e., orbit determination and trajectory control) of this spacecraft, but assume that it is kept on track and is always relatively close to the periodic orbit. Some practical aspects of navigating such a spacecraft are discussed in Scheeres et al. (1999).

## Relative Motion of the Spacecraft

In our ideal problem, we assume that the first spacecraft is following a periodic halo orbit and the second spacecraft is on a neighboring trajectory. Since we desire the two spacecraft to maintain a close relative distance to each other, we assume that the second spacecraft is not on a neighboring periodic orbit, as this would imply a different orbit period

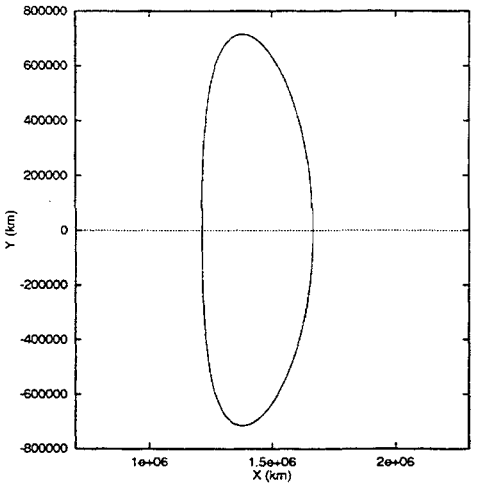


Figure 1: Halo orbit trajectory projected into the $x$-$y$ plane.

and hence a secular increase in their relative distance. Rather, the second spacecraft is assumed to be in a non-periodic orbit in the vicinity of the first spacecraft.

### Linearized Dynamics

The first spacecraft has a trajectory defined as $\mathbf{R}(t; \mathbf{R}_o, \mathbf{V}_o)$, $\mathbf{R}(t+T) = \mathbf{R}(t)$, where $T$ is the period of motion. Naturally, the velocity of the spacecraft, $\mathbf{V}(t; \mathbf{R}_o, \mathbf{V}_o)$, is also periodic with period $T$. The second spacecraft has its own trajectory defined with position and velocity $\mathbf{r}(t; \mathbf{r}_o, \mathbf{v}_o)$ and $\mathbf{v}(t; \mathbf{r}_o, \mathbf{v}_o)$. If the distance between the two spacecraft is assumed to be relatively small, then the trajectory of the second spacecraft can be approximated using linearized equations of motion. Define $\mathbf{x} = [\mathbf{r}, \mathbf{v}]$ and $\mathbf{X} = [\mathbf{R}, \mathbf{V}]$. Then the difference between these states is $\delta\mathbf{x}$, which is assumed to be "small" relative to the state $\mathbf{X}$. The dynamics of $\delta\mathbf{x}$ are derived as:

$$\delta\mathbf{x} = \mathbf{x} - \mathbf{X} \quad (4)$$

$$\delta\dot{\mathbf{x}} = \dot{\mathbf{x}} - \dot{\mathbf{X}} \quad (5)$$

$$= \mathbf{F}(\mathbf{X} + \delta\mathbf{x}) - \mathbf{F}(\mathbf{X}) \quad (6)$$

$$= \mathbf{F}(\mathbf{X}) + \frac{\partial \mathbf{F}}{\partial \mathbf{X}}\delta\mathbf{x} + \ldots - \mathbf{F}(\mathbf{X}) \quad (7)$$

$$\sim A(t)\delta\mathbf{x} \quad (8)$$

$$A(t) = \frac{\partial \mathbf{F}}{\partial \mathbf{X}} \quad (9)$$

$$A(t+T) = A(t) \quad (10)$$

where $\mathbf{F}(\mathbf{X})$ is the dynamics function corresponding to Equations 1 – 3. The solution for relative motion

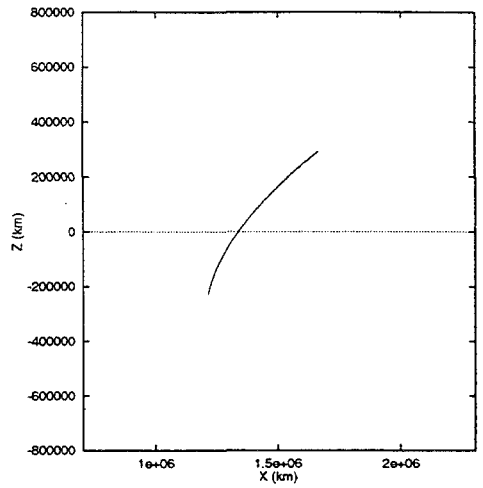


Figure 2: Halo orbit trajectory projected into the $x$-$z$ plane.

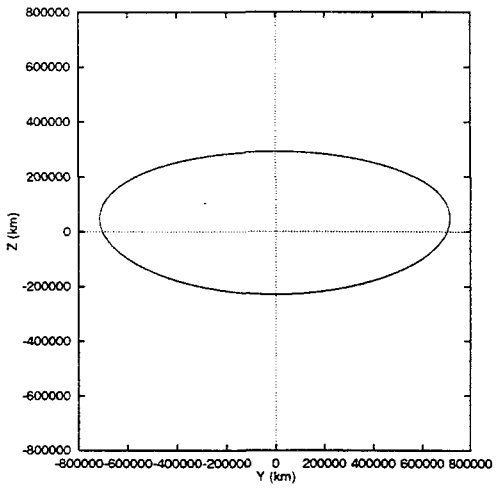


Figure 3: Halo orbit trajectory projected into the $y$-$z$ plane.

can then be expressed as:

$$\delta \mathbf{x} = \Phi(t, t_o)\delta \mathbf{x}_o \quad (11)$$

$$\Phi(t, t_o) = \frac{\partial \mathbf{X}(t; \mathbf{X}_o)}{\partial \mathbf{X}_o} \quad (12)$$

$$\dot{\Phi}(t, t_o) = A(t)\Phi(t, t_o) \quad (13)$$

$$\Phi(t_o, t_o) = I \quad (14)$$

where $\Phi$ is the state transition matrix, computed about the periodic orbit, and $\delta \mathbf{x}_o$ is the initial offset of the spacecraft from the periodic orbit.

## Long-Term Relative Motion

For the case of long-term motion, i.e., spacecraft motion on the order of the orbit period or longer, the state transition matrix can be written as the product of two matrices by application of Floquet's theorem (Cesari, pp. 55 – 59):

$$\Phi(t, t_o) = P(t - t_o)e^{(t-t_o)D} \quad (15)$$

where $P$ is a periodic matrix of period $T$ and $D$ is a constant matrix which has, as its eigenvalues, the characteristic exponents of the periodic orbit over one orbital period. As noted earlier, our periodic halo orbit has one pair of hyperbolic characteristic exponents and two circulation frequencies, one equal to the orbit period and one slightly longer. Due to the presence of the unstable manifold, uncontrolled relative motion will rapidly move away from the vicinity of the periodic orbit.

If we wish the spacecraft to maintain a long-term trajectory in the neighborhood of the periodic orbit we must place it in the center manifold of the periodic orbit, defined as the space of orbits that do not lie along the hyperbolic manifolds of the periodic orbit. A spacecraft in such an orbit will naturally circulate about the periodic orbit in a quasi-periodic orbit, its trajectory winding onto a torus that encloses the periodic orbit in 3-dimensional space. Such a relative orbital configuration is attractive as, depending on the initial conditions given to the spacecraft, an ensemble of spacecraft distributed along such initial conditions may serve a useful purpose as a constellation of spacecraft (Barden and Howell 1998). Unfortunately, the practical implementation of such a family of orbits is extremely difficult, requiring precision placement and control of the spacecraft at all points along the trajectory, as the center manifold is itself an unstable object.

## Short-Term Relative Motion

For practical considerations we may instead concern ourselves with the relative dynamics of the spacecraft over a time much less than the orbital period. While, in principle, the description of relative motion given in Equation 15 holds true, it does not give us a direct indication of relative motion over shorter time periods.

We can represent the state transition matrix of the periodic orbit over one period as the product of mappings over much shorter time intervals within the period of motion:

$$\Phi(t_o + T, t_o) = \prod_{i=1}^{N} \Phi\left(t_o + \frac{T}{N}i, t_o + \frac{T}{N}(i-1)\right) \quad (16)$$

Where the mapping over a time interval $\Delta t$ is represented as $\Phi(t_i + \Delta t, t_i)$ and conforms to the equation:

$$\dot{\Phi}(t_i + \delta t, t_i) = A(t_i + \delta t)\Phi(t_i + \delta t, t_i) \quad (17)$$

$$0 \leq \delta t \leq \Delta t \ll T \tag{18}$$

For $\Delta t$ small enough we can expand $A(t)$ in a Taylor Series expansion, yielding:

$$A(t_i + \delta t) = A(t_i) + A'(t_i)\delta t + \dots \tag{19}$$

For our problem, we find that the force partial matrix $A(t)$ does not vary strongly over time, meaning that the time interval $\Delta t$ can be chosen small enough to ensure that $||A(t_i)|| \gg ||A'(t_i)\Delta t||$. With this restriction, we find that the state transition matrix differential equation can be approximated over short time intervals as:

$$\dot{\Phi}(t_i + \delta t, t_i) = A(t_i)\Phi(t_i + \delta t, t_i) + \dots \tag{20}$$

giving a time invariant system at leading order. Thus, the solution can be expressed as:

$$\Phi(t_i + \delta t, t_i) \sim e^{A(t_i)\delta t} + \dots \tag{21}$$

$$\sim I + A(t_i)\delta t + \dots \tag{22}$$

where, since the time interval is chosen to be small, we neglect higher orders of the exponential expansion.

The relative motion of the spacecraft can then be characterized over a short period of time by the eigenvalues and eigenvectors of the exponential map, defined from the equation:

$$\Phi \mathbf{u} = \lambda \mathbf{u} \tag{23}$$

or equivalently:

$$(\lambda I - \Phi)\,\mathbf{u} = 0 \tag{24}$$

where $\lambda$ is the eigenvalue and $\mathbf{u}$ is the eigenvector. Using Equation 22 this can be reduced to:

$$\left[\frac{(\lambda - 1)}{\delta t} I - A(t_i)\right] \mathbf{u} = 0 \tag{25}$$

For a time invariant system the eigenvalue of the state transition matrix, $\lambda$, in Equation 24 is equal to $e^{\gamma(\delta t)}$, where $\gamma$ is the characteristic exponent of the system. Thus, the eigenvalue of Equation 25 can be approximated as:

$$\gamma \sim \lim_{\delta t \to 0} \frac{\lambda - 1}{\delta t} \tag{26}$$

From this sequence of approximations we see that the relative motion of the S/C over a short time span centered at time $t_i$ can be understood by analyzing the eigenvalues and eigenvectors of the matrix $A(t_i)$. Such an analysis resembles the analysis of an equilibrium point carried out at each time $t_i$.

Given the base periodic orbit, the characteristic exponents and frequencies of $A(t_i)$ can be computed at each point in time, and are shown in Figure 4. We see that for our base periodic orbit the structure is consistent, having a pair of hyperbolic roots and two pair of oscillatory roots at each moment in time. The generalization of this result to the family of halo orbits has not been performed as of yet. In Figure 5 we show the characteristic exponents of the numerically computed maps $\Phi(t_i + \Delta t, t_i)$ for decreasing values of $\Delta t$. Comparison of the characteristic exponents with the exponents derived at each instant of time clearly shows that the actual characteristic exponents converge to the "instantaneous" characteristic exponents as $\Delta t$ shrinks.

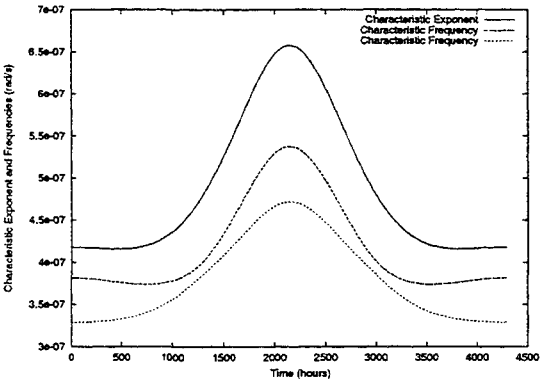


Figure 4: Instantaneous characteristic exponents and frequencies of the of the periodic orbit over one period of motion.

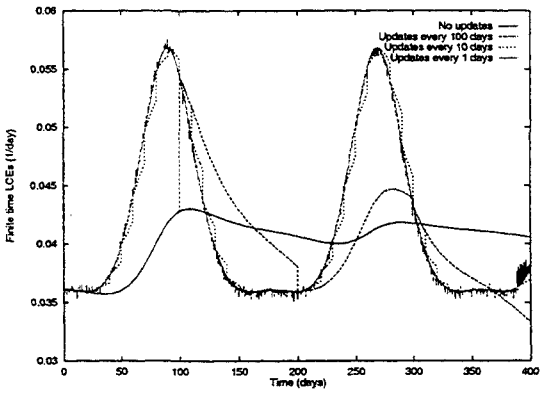


Figure 5: Characteristic exponents of the unstable hyperbolic mode of the periodic orbit computed for the state transition maps $\Phi(t_o + i\Delta t, t_o + (i-1)\Delta t)$, $\Delta t = T/N$, $T$ equal to the orbit period. The exponents are computed for increasing values of $N$. It is clear that as $N$ becomes large (and $\Delta t$ small) that the exponents converge to the instantaneous values of the map.

In deriving our control law we will use these "short-

term" dynamics to guide our thinking. It is a fairly natural approach, since a precursor for a spacecraft to diverge from the periodic orbit over a longer time span will be for it to diverge from the periodic orbit over a shorter time span. Thus, we can think of relative motion along the unstable manifolds to be a precursor to motion along the unstable manifold of the full orbit, as defined by Floquet theory. Note, that the full orbit may still be unstable, even if the instantaneous map is stable at each time step. We will see examples of this later.

## Stabilizing the Relative Motion

A control law is formulated which can stabilize the relative motion of the spacecraft. We first derive the control by focusing on stabilizing the "short-term" dynamics, as described previously. We then show that this "local stabilization" can also stabilize the long-term relative motion of the spacecraft.

### Local Stabilization

Neglecting the larger issue of long-term stability for now, we focus on stabilizing the relative motion between the two spacecraft over short time spans. There are many different approaches that can be taken here, depending on what form we wish the resulting motion to take. For the constellation applications we are considering it would be most beneficial if the relative control between the spacecraft would allow for stable oscillations, such as are found in the center manifold of an orbit. If the control law can give such solutions, then we have considerable freedom to choose and change the relative motion of the spacecraft throughout the orbit. Specifically, if the control law reduces the relative motion to oscillatory motion, then a variety of motions can be implemented by proper choice of the intial conditions. Additionally, the application of one or two impulsive maneuvers can excite a different aspect of the relative motion and change the dynamics of the constellation. Technically, we wish to choose a control law which will establish Lyapunov stability of the relative motion.

We propose a specific control law which can provide Lyapunov stability of our local, short time motion for a sufficiently large gain constant. To implement this control at a given time $t_i$ we evaluate the local eigenstructure of the matrix $A(t_i)$ and find the characteristic exponents of the hyperbolic motion, $\pm\sigma(t_i)$, and find the eigenvectors that define the stable and unstable manifolds of this motion, $\mathbf{u}_{\pm}(t_i)$, where the $+$ denotes the unstable manifold and the $-$ denotes the stable manifold. To stabilize the motion we then assume that the relative position vector of the spacecraft is projected into the stable and unstable manifolds, and that this projection is multiplied by a gain constant and an acceleration of this magnitude is applied along the stable and unstable manifolds, respectively. Thus, the control acceleration which we apply is:

$$\mathcal{T}_c = -\sigma^2 G \left[\mathbf{u}_+\mathbf{u}_+^T + \mathbf{u}_-\mathbf{u}_-^T\right]\delta\mathbf{r} \tag{27}$$

where $\sigma^2 G$ is the gain constant and $\delta\mathbf{r}$ is the measured relative position vector between the two spacecraft (i.e., the offset between the periodic orbit and the 2nd spacecraft). We note that the eigenvalues $\pm\sigma(t_i)$ and eigenvectors $\mathbf{u}_{\pm}(t_i)$ are well-defined periodic functions of time, with period equal to the base periodic orbit.

Given this specific control law we can reformulate the relative dynamics of our system, taking advantage of the Lagrangian structure of the equations of motion. Denote the linearized equations of motion for relative motion as:

$$\delta\mathbf{r}'' - 2\omega J\delta\mathbf{r}' - V_{rr}\delta\mathbf{r} = 0 \tag{28}$$

$$J = \begin{bmatrix} 0 & 1 & 0 \\ -1 & 0 & 0 \\ 0 & 0 & 0 \end{bmatrix} \tag{29}$$

where $\omega$ is the rotation rate of the coordinate frame and $V_{rr}(t_i)$ is the second partial of the force matrix evaluated along the periodic orbit, making it a time-varying, periodic matrix as well. Then, the eigenvalues and eigenvectors that we use in our control scheme are computed from:

$$\left[\sigma^2 I \mp 2\omega\sigma J - V_{rr}\right]\mathbf{u}_{\pm} = 0 \tag{30}$$

Implementing the control acceleration of Equation 27 into Equation 28 has the effect of modifying our potential force contributions to the linear system:

$$\delta\mathbf{r}'' - 2\omega J\delta\mathbf{r}' - \left\{V_{rr} - \sigma^2 G\left[\mathbf{u}_+\mathbf{u}_+^T + \mathbf{u}_-\mathbf{u}_-^T\right]\right\}\delta\mathbf{r} = 0 \tag{31}$$

This control law maintains the Hamiltonian nature of the problem, and provides local stability if the gain constant $G$ is chosen sufficiently large. In the Appendix we show that this control law can always stabilize a time-invariant, hyperbolic unstable 2 degree of freedom Hamiltonian system, and give a heuristic justification for scaling our gain constant by the characteristic exponent squared.

The control law just consists of a "reshaping" of the local force structure by proper application of thrusting. We shall see that since the magnitude of these forces is rather small in the vicinity of the libration points the amount of acceleration needed to implement this control is also relatively small and

could be provided by a low-thrust propulsion system in many cases.

## Long-Term Stability

Equation 31 generalizes to the relative motion of our spacecraft over longer time spans as well, as the spectrum of the dynamics, Equation 30, is well defined at each moment and as the stability type of the local motion does not change over the entire orbit. Thus, the eigenvalues $\pm\sigma$ and eigenvectors $\mathbf{u}_\pm$ are all well defined functions of time.

Computation of Stability Stabilization of the relative motion over short time spans is nice, but does not necessarily guarantee that the motion of the spacecraft will be stable over longer time spans. Technical conditions for which such a time periodic system may be stable are discussed in greater detail in Cesari (1963). However, these mathematical conditions, even if definite, will in general not be easily applied to the current system where we have fully general motion in three dimensions defined numerically and a linear map that changes significantly with time. The stability of the system can be evaluated, however, by application of Floquet theory and numerical integration.

Again, since the eigenvalues and eigenvectors used in the feedback control are functions only of the periodic orbit, they are in turn periodic, making the linear dynamical system defined in Equation 31 time periodic. Also, since the control forces are only a function of position, and are in principle derivable from a potential function, we see that the control law does not change the conservative structure of the dynamics. Thus, the characteristic exponents of the linear map over one period will follow the general rules for conservative, Hamiltonian systems.

The algorithm which we apply is given, in brief, as follows. The periodic orbit and its accompanying state transition matrix, modified by introduction of the stabilization control, is numerically integrated over one period of motion. At each time step the spectrum of the open loop system is computed and fed into Equation 31. The gain constant $G$ is a free parameter that is specified at the start of the integration. The modified, time-varying matrix $\tilde{A}(t)$ used in the state transition matrix computation is specified as:

$$\tilde{A}(t) = \left[\begin{array}{c|c} 0 & I \\ \hline V_{rr} - \sigma^2 G\left[\mathbf{u}_+\mathbf{u}_+^T + \mathbf{u}_-\mathbf{u}_-^T\right] & 2\omega J \end{array}\right] \quad (32)$$

The resulting state transition matrix is denoted as $\tilde{\Phi}(t_o + t, t_o)$, and the monodromy matrix evaluated over one period of motion is then $\tilde{\Phi}(t_o + T, t_o)$. The minimum computation then consists of the integration of the periodic orbit (6 equations) plus the integration of the modified state transition matrix (36 equations). The integration was performed using a variable step size RK78 algorithm, with error control applied to the entire set of 42 equations. As the gain is increased, it is the numerical integration of $\tilde{\Phi}$ that controls the step size choice, and hence it is most convenient to carry along the computation of the periodic orbit, as it and the spectrum of its local motion will then be evaluated at the appropriate time for inclusion in the $\tilde{\Phi}$ computation. This is found to be simpler than pre-computing and storing the periodic orbit and its local stability characterization.

The stability of the closed loop system can then be evaluated by computing the eigenvalues, $\mu$, of this map:

$$\left[\mu I - \tilde{\Phi}(t_o + T, t_o)\right]\mathbf{v} = 0 \quad (33)$$

As detailed in Marchal (pp 171–173) the eigenvalues of this map must occur in complex conjugate pairs and in inverse pairs, meaning that for every complex eigenvalue $\mu$, its conjugate $\bar{\mu}$ must also be an eigenvalue, and that for every eigenvalue with magnitude different than 1, $|\mu| \neq 1$, there must also be an eigenvalue of magnitude $1/|\mu|$. Stability of this system occurs when all the eigenvalues have unit magnitude, i.e., reside on the unit circle in the complex plane and have the form $\mu = e^{\pm i\theta}$. Conversely, an unstable map will either have a pair of multipliers along the real axis, of the form $\pm(\rho, 1/\rho)$, or will have a foursome of complex multipliers that lie off of the unit circle and have the form $\rho e^{\pm i\theta}$, $(1/\rho)e^{\pm i\theta}$. Either of these modes will lead to exponentially unstable relative motion between the spacecraft.

For the case of a completely stable map, there are three pairs of eigenvalues, each pair characterized by the angle $\theta_i, i = 1, 2, 3$. This angle denotes the total winding angle of the mode about the periodic orbit, modulus $2\pi$. Taken together, they define a quasi-periodic orbit with three seperate "average" periods over one periodic orbit. For the general characterization of these oscillation modes we can consider the angles to be functions of time along the orbit, $\theta_i(t)$, with their final values computed from the monodromy map being $\theta_i = \mathrm{mod}(\theta_i(T), 2\pi)$. Unfortunately, there is no direct way to extract $\theta_i(t)$ from the numerically computed monodromy map. This is an item of interest, however, as the frequency of these stable motions will change with the gain constant $G$, and can be much larger than the periodic orbit frequency, meaning that a spacecraft having

motion along this mode can encircle the periodic orbit several times over one period of the base orbit. Thus, defining and computing these mean frequencies is of practical interest for the relative motion. Ideally, we compute them as:

$$\bar{\omega}_i = \frac{\theta_i(T)}{T} \quad (34)$$

$$= 2\pi N_i + \theta_i \quad (35)$$

We find that the number $N_i$ can be estimated from the time history of the spectrum of the state transition matrix $\tilde{\Phi}$ by counting the zero crossings of the stable modes, however this approach is not always well-defined as the intermediate spectrum of the matrix is not always stable. A different approach to this computation, that works when the numbers $N_i$ become relatively large, is to estimate the angle $\theta_i(t)$ by performing the quadrature:

$$\tilde{\theta}_i(t) = \int_0^t \tilde{\omega}_i(t)dt \quad (36)$$

where the frequency $\tilde{\omega}_i(t)$ is defined as an instantaneous characteristic frequency of the linear matrix $\tilde{A}(t)$, which has been stabilized by our application of local control. We find that reasonable estimates of the mean frequency of the stable modes of the relative motion can be found from this quadrature. Improvements to this approach will be investigated in the future.

Stability as a function of Gain As formulated, there is only one parameter for the controller, the gain constant $G$. We see that, as this constant is increased, the nature of the linear dynamics changes. For values of $G$ when the monodromy matrix is stable, the space of all relative motions can be found by computing the characteristic frequencies and eigenvectors of the matrix. Motion under this map will in general lie on quasi-periodic tori surrounding the periodic orbit – somewhat similar to motion in the center manifold but with additional frequencies to choose from and elimination of instability concerns. To give insight into these possible modes of motion we evaluate the characteristics of the monodromy matrix as $G$ is increased.

For $G < 1.17$ the control law has insufficient authority to stabilize the local motion at every time along the periodic motion, meaning that there are time intervals where the spectrum of $\tilde{A}(t)$ is not completely stable. We note that the monodromy matrix is also found to be unstable for this situation. Only for values of $G$ greater than 1.17 is the instantaneous motion stable over the entire periodic orbit. However, we note that stability of the local motion does not guarantee the stability of the monodromy matrix. And, in fact, we find that the monodromy map does not become stable until the gain $G$ reaches a value of 2.19.

In general, we find that the map is stable for gains greater than this value. There are exceptions corresponding to resonances between the oscillation modes and with the periodic orbit period. However, in analogy to the Mathieu equation, as the gain becomes larger the size of these instability intervals become small. The most significant intervals of instability occur for relatively low values of gain. The first two appear in the interval $3.47 \leq G \leq 5.21$, which corresponds to single and double resonances with the orbital period, resulting in one pair of multipliers of the form $\rho_1$, $1/\rho_1$, and another of the form $-\rho_2$ and $-1/\rho_2$. The next interval of instability is $5.92 \leq G \leq 6.10$, where two of the modes have a resonance, one having twice the period of the other, and resulting in a complex set of four multipliers.

We note that the magnitude of the multipliers in these intervals are "small", the maximum multiplier in the above intervals being less than 1.1 over one orbit period (corresponding to a characteristic time greater than 5 years). This is especially small as compared to the original instability of the periodic orbit which has a characteristic time of 23 days. In many cases these instabilities would not appreciably hamper the use of this relative control. Such intervals of instability are expected, and in general correspond to the eigenvalues of the monodromy map intersecting on the unit circle (see Marchal for a detailed discussion of possible stability transitions). As noted in Marchal, the presence of oscillatory, linear stability does not imply non-linear stability of the relative orbits. However, we are assured that any non-linear instabilities will not grow exponentially, but will only grow, at most, as a polynomial in time. For practical considerations, this implies that such instabilities should be controllable by standard navigation practices over time.

As the gain of the control loop increases, we find that the mean oscillation frequencies of the system defined earlier, $\bar{\omega}_i$, change as well. For our system, one of these mean frequencies remains relatively constant and is consistently less than the periodic orbit frequency ($2\pi/T$). This oscillation mode is associated most strongly with "out-of-plane" motion along the $z$ axis of the system, and related to the initial stable oscillation mode of the uncontrolled relative motion. While the control loop does influence this stable oscillation mode, it never causes it to stray

far from its original value.

Conversely, the mean frequency of the other two oscillation modes increase, in general, as the square root of the gain $G$. One of these modes originates from the original open loop oscillation of period $T$, while the other is created when the closed loop control removes the hyperbolic manifolds. By specifying the control gain $G$ the "natural dynamics" of the relative motion can be modified, causing the relative motion between the spacecraft to follow different paths. By characterizing the oscillation planes of these motions over time it is possible to distribute a constellation of spacecraft so that they, as a group, are oriented toward a specific direction. For large values of $G$ these mean frequencies are approximately equal to $\sigma\sqrt{G}$ and $\sigma\sqrt{G}/2$, where $\sigma \sim 4.7 \times 10^{-7}/s$ is the characteristic exponent of the open-loop unstable periodic orbit. In terms of oscillation period, these are approximately $154/\sqrt{G}$ days and $309/\sqrt{G}$ days.

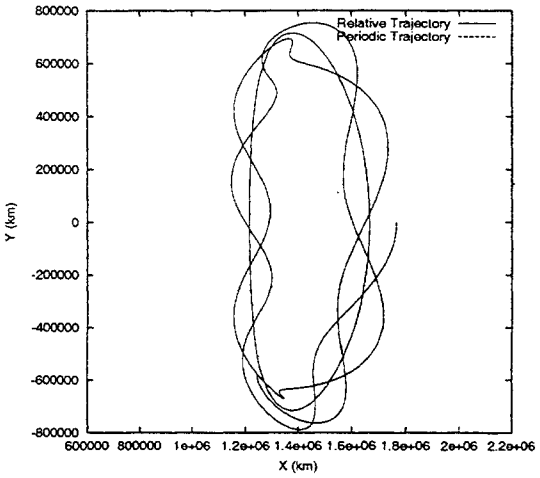


Figure 6: Controlled and halo orbit trajectory projected into the $x$-$y$ plane. Control gain of 10 is applied, with an initial position offset of $1 \times 10^5$ km.

Stabilizing non-linear motion The linear stability of the control law for our halo orbit having been established numerically, it is of interest to verify that it can actually stabilize a non-linear trajectory about a periodic orbit. To verify this, we apply the control acceleration given in Equation 27 to the full equations of motion of a spacecraft moving according to Equations 1 – 3. The initial conditions of this motion are denoted as an offset from the initial conditions of the periodic orbit at the initial time, and the relative position between the trajectory and the periodic orbit, needed for the control, is computed as the vector difference between the two solutions at each moment in time. This formulation is entirely consistent, as the computed difference is equivalent to the measured difference between the two spacecraft, and the local stability computations are based on the periodic orbit, which can in principle be computed on-board the controlled spacecraft.

To push the control law to a somewhat extreme condition, we gave the spacecraft an initial position offset from the periodic orbit of $1 \times 10^5$ km with gains of 10 and 100. The resulting trajectories are shown in Figures 6 – 11. Each of these trajectories is integrated over 400 days, which is more than two periods of the periodic orbit. We note that our control law is able to maintain the stable relative motion over this time frame. It is significant to note that the computation of the periodic orbit itself over this length of time is non-trivial, due to the strength of its instability.

We also note that the control law is being applied in a region where non-linearities dominate the system. In Figure 12 we show a plot of the motion relative to the periodic orbit for a case with an initial position offset of $5 \times 10^5$ km and control gain of 10, projected into the $y$ and $z$ coordinate planes. Also shown is the linear solution to Equation 31, started with the same value of offset but obviously following a different trajectory as compared to motion in the "real" system. This gives an indication that our control law remains robust when the relative motion is no longer well defined with the linear equations of motion.

## Control Implementation

Having shown that our control law stabilizes relative motion and is robust when applied to fully non-linear motion, it is necessary to compute the thrust needed to properly apply the control. In our computations we keep track of the total "$\Delta V$" expended by performing the quadrature:

$$\Delta V(t) = \int_0^t |T_c| dt \tag{37}$$

The actual time history of the instantaneous thrust and accumulated $\Delta V$ changes as the gain and initial conditions are varied. An estimate of the necessary thrust level at any instant can be given by the relation:

$$T_c \sim 2\sigma^2 GR \tag{38}$$

where $R$ is the amplitude of the relative motion of the spacecraft in the $x$-$y$ plane, $\sigma \sim 4.7 \times 10^{-7}/s$ is the characteristic exponent of our periodic orbit,

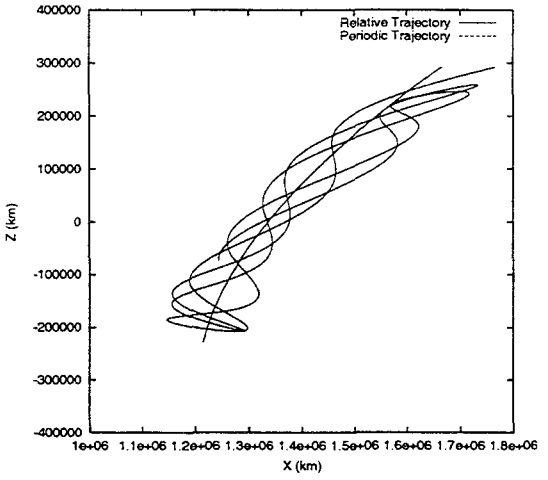


Figure 7: Controlled and halo orbit trajectory projected into the $x$-$z$ plane. Control gain of 10 is applied, with an initial position offset of $1 \times 10^5$ km.

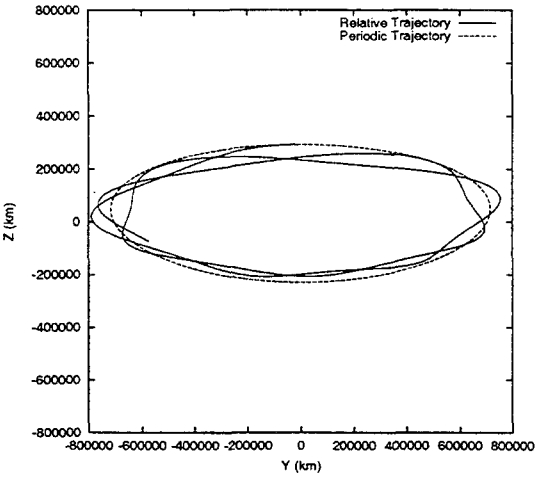


Figure 8: Controlled and halo orbit trajectory projected into the $y$-$z$ plane. Control gain of 10 is applied, with an initial position offset of $1 \times 10^5$ km.

and $G$ is the control gain. Thus we see that the thrust will scale as $0.44GR$ nm/s$^2$.

To apply a gain of 100 (oscillation periods of 15 and 31 days) with a relative constellation size of 1000 km requires a thrust of 44 micrometers/s$^2$. For a 100 kg spacecraft, this translates into a thrust of 4.4 milli-Newtons. For a low-thrust ion engine with a characteristic velocity of 30 km/s over a 2 year mission, the resulting mass fuel fraction used is on the order of 5%.

To successfully apply the control law we must measure the relative position along the directions of stable and unstable motion. Radial distance and radial rate can be measured with a ranger and Doppler extractor (we assume near-continuous communication between the spacecraft in support of their scientific mission). If multiple receivers are placed on the spacecraft, the relative orientation of the spacecraft can be determined and, by processing the inertially measured attitude, the relative position of the spacecraft can be determined at each moment. In Scheeres et al. (1999) it was found that the orbit uncertainty of a single spacecraft in an unstable halo orbit tended to be minimized along the local stable and unstable manifolds of the trajectory. A similar result for the relative orbit determination between two spacecraft would support the potential feasibility of our proposed approach to trajectory control. Studies of this effect will be made in the future.

## Conclusions

In this paper we address issues concerned with the control of formation flying spacecraft in unstable orbital environments. As a nominal case we consider formation flying spacecraft in an unstable halo orbit about the Earth-Sun libration point. The relative dynamics of these spacecraft are considered along with the practical computation of relative orbits and the measurement and dynamics of relative orbit uncertainty between the spacecraft. We find a family of simple control laws that stabilize the relative motion and appear to be very robust. The cost and feasibility of implementing these control laws are addressed and found to be reasonable.

## Acknowledgements

The work described here was funded by the TMOD Technology Program by a grant from the Jet Propulsion Laboratory, California Institute of Technology which is under contract with the National Aeronautics and Space Administration.

## Appendix

We first consider stabilization of a simple, 1DOF, hyperbolic unstable motion. The generic form for this case is:

$$\ddot{r} - \sigma^2 r = 0 \tag{39}$$

where $\sigma$ is the characteristic exponent of the unstable system. In this case an intuitively obvious stabilization is to apply a position feedback acceleration of the form $-Kr$, yielding the modified system:

$$\ddot{r} - (\sigma^2 - K)r = 0 \tag{40}$$

Now, an obvious condition for stability is $K > \sigma^2$, or rewriting $K = \sigma^2 G$, the stability condition becomes $G > 1$. This simple result motivates us to

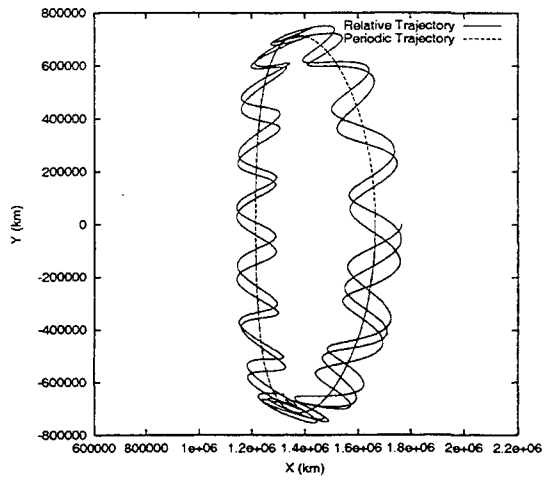


Figure 9: Controlled and halo orbit trajectory projected into the $x$-$y$ plane. Control gain of 100 is applied, with an initial position offset of $1 \times 10^5$ km.

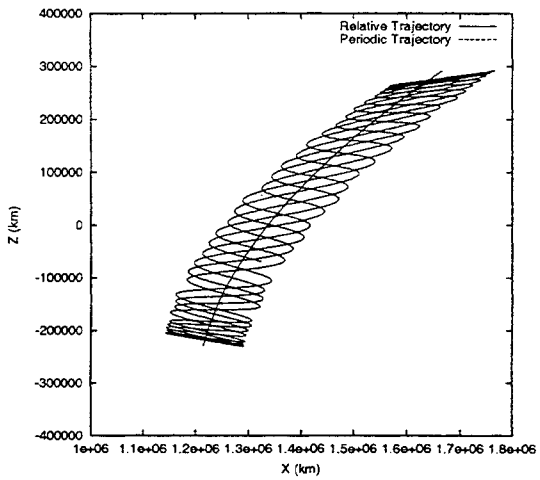


Figure 10: Controlled and halo orbit trajectory projected into the $x$-$z$ plane. Control gain of 100 is applied, with an initial position offset of $1 \times 10^5$ km.

scale our feedback gain by the square of the local characteristic exponent.

Next consider application of our local stabilization control scheme to an unstable hyperbolic point in a rotating 2DOF frame. The open loop dynamics are specified by the linear equation:

$$\begin{bmatrix} \delta x'' \\ \delta y'' \end{bmatrix} - 2\omega \begin{bmatrix} 0 & 1 \\ -1 & 0 \end{bmatrix} \begin{bmatrix} \delta x' \\ \delta y' \end{bmatrix} - \begin{bmatrix} V_{xx} & V_{xy} \\ V_{xy} & V_{yy} \end{bmatrix} \begin{bmatrix} \delta x \\ \delta y \end{bmatrix} = 0 \quad (41)$$

The characteristic equation for this system is:

$$\lambda^4 + \left[4\omega^2 - V_{xx} - V_{yy}\right]\lambda^2 + V_{xx}V_{yy} - V_{xy}^2 = 0 \quad (42)$$

For a singly hyperbolic unstable system we can assume, in general, that

$$V_{xx}V_{yy} - V_{xy}^2 < 0 \quad (43)$$

The hyperbolic characteristic exponents of the system are computed from:

$$\sigma^2 = -\frac{1}{2}\left[4\omega^2 - V_{xx} - V_{yy}\right] + \frac{1}{2}\sqrt{\left(4\omega^2 - V_{xx} - V_{yy}\right)^2 - 4\left(V_{xx}V_{yy} - V_{xy}^2\right)} \quad (44)$$

which is guaranteed to be positive if the inequality in Equation 43 holds. The corresponding eigenvectors will be of the form:

$$\mathbf{u}_\pm = \frac{1}{\sqrt{1+u_\pm^2}} \begin{bmatrix} 1 \\ u_\pm \end{bmatrix} \quad (45)$$

$$u_\pm = \frac{\sigma^2 - V_{xx}}{V_{xy} \pm 2\omega\sigma} \quad (46)$$

$$= \frac{V_{xy} \mp 2\omega\sigma}{\sigma^2 - V_{yy}} \quad (47)$$

The gain matrix that is added to the left hand side of Equation 41 (corresponding to Equation 32) is:

$$\sigma^2 G \left[\begin{array}{c|c} \frac{1}{1+u_+^2} + \frac{1}{1+u_-^2} & \frac{u_+}{1+u_+^2} + \frac{u_-}{1+u_-^2} \\ \hline \frac{u_+}{1+u_+^2} + \frac{u_-}{1+u_-^2} & \frac{u_+^2}{1+u_+^2} + \frac{u_-^2}{1+u_-^2} \end{array}\right] \quad (48)$$

Reforming the characteristic equation for this case yields:

$$\lambda^4 + \left[4\omega^2 - \tilde{V}_{xx} - \tilde{V}_{yy}\right]\lambda^2 + \tilde{V}_{xx}\tilde{V}_{yy} - \tilde{V}_{xy}^2 = 0 \quad (49)$$

where

$$\tilde{V}_{xx} = V_{xx} - \sigma^2 G\left[\frac{1}{1+u_+^2} + \frac{1}{1+u_-^2}\right] \quad (50)$$

$$\tilde{V}_{yy} = V_{yy} - \sigma^2 G\left[\frac{u_+^2}{1+u_+^2} + \frac{u_-^2}{1+u_-^2}\right] \quad (51)$$

$$\tilde{V}_{xy} = V_{xy} - \sigma^2 G\left[\frac{u_+}{1+u_+^2} + \frac{u_-}{1+u_-^2}\right] \quad (52)$$

To guarantee linear stability of this system requires that three conditions be met:

$$\left[4\omega^2 - \tilde{V}_{xx} - \tilde{V}_{yy}\right] > 0 \quad (53)$$

$$\tilde{V}_{xx}\tilde{V}_{yy} - \tilde{V}_{xy}^2 > 0 \quad (54)$$

$$\left[4\omega^2 - \tilde{V}_{xx} - \tilde{V}_{yy}\right]^2 - 4\left[\tilde{V}_{xx}\tilde{V}_{yy} - \tilde{V}_{xy}^2\right] > 0 \quad (55)$$

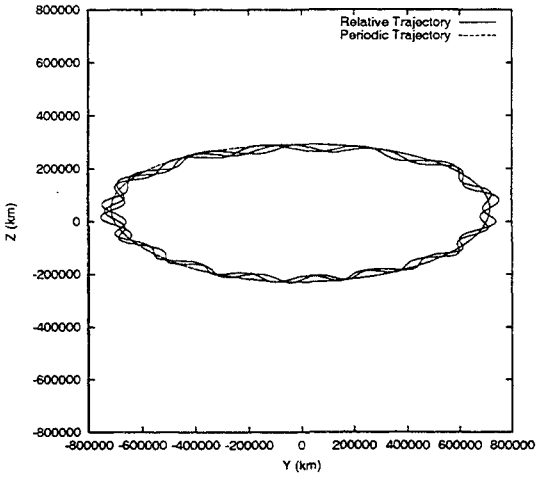


Figure 11: Controlled and halo orbit trajectory projected into the $y$-$z$ plane. Control gain of 100 is applied, with an initial position offset of $1 \times 10^5$ km.

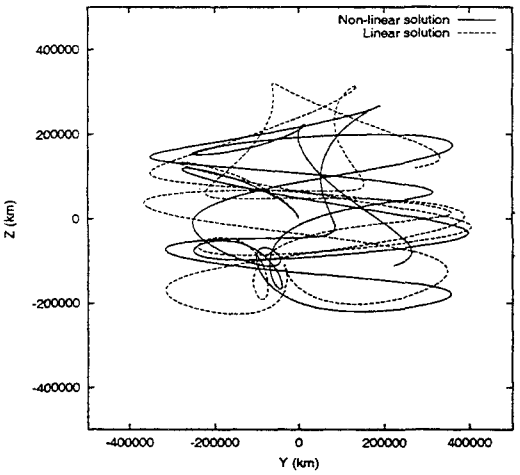


Figure 12: The non-linear and linear trajectory computations relative to the periodic orbit, projected into the $y$-$z$ plane. Control gain of 10 is applied, with an initial position offset of $5 \times 10^5$ km.

We note that Condition 53 can be rewritten as:

$$4\omega^2 - V_{xx} - V_{yy} + 2\sigma^2 G \;>\; 0 \tag{56}$$

which can be satisfied for large enough $G$. Next, expanding Condition 54 results in the form:

$$\begin{aligned} &\sigma^4 G^2 (u_+ - u_-)^2 \\ -\sigma^2 G &\left[ \left(1+u_-^2\right) \left\{ u_+^2 V_{xx} + V_{yy} - 2u_+ V_{xy} \right\} \right. \\ &+ \left(1+u_+^2\right) \left\{ u_-^2 V_{xx} + V_{yy} - 2u_- V_{xy} \right\} \Big] \\ &+ \left(1+u_+^2\right)\left(1+u_-^2\right)\left(V_{xx}V_{yy} - V_{xy}^2\right) \;>\; 0 \end{aligned} \tag{57}$$

Again, we see that $G$ can be chosen large enough to guarantee stability. Finally, we note that Condition 55 can be rewritten as

$$\begin{aligned} 8\omega^2 &\left[ 2\omega^2 - \left( \tilde{V}_{xx} + \tilde{V}_{yy} \right) \right] + \\ &\left( \tilde{V}_{xx} - \tilde{V}_{yy} \right)^2 + 4\tilde{V}_{xy}^2 \;>\; 0 \end{aligned} \tag{58}$$

which, on inspection, reduces to the sufficient condition

$$2\omega^2 - \tilde{V}_{xx} - \tilde{V}_{yy} \;>\; 0 \tag{59}$$

or equivalently

$$2\omega^2 - V_{xx} - V_{yy} + 2\sigma^2 G \;>\; 0 \tag{60}$$

for which $G$ can always be chosen large enough to stabilize. Should this condition be true, then Condition 56 follows trivially. Thus we note that our proposed control law can always stabilize the hyperbolic unstable equilibrium point for large enough $G$. The attractiveness of this controller is that it has a natural specification for our time-varying system at each moment of time and depends only on the estimate of relative position between the spacecraft and an estimate of the position of the spacecraft on the nominal periodic orbit.

# References

Barden, B.T., K.C. Howell, "Fundamental Motions Near Collinear Libration Points and Their Transitions," JAS 46: 361–378, 1998.

Cesari, L., Asymptotic Behavior and Stability Problems in Ordinary Differential Equations, 2nd Ed., Academic Press, 1963.

Gomez, G., J. Masdemont, C. Simo, "Quasihalo Orbits Associated with Libration Points," JAS 46: 135–176, 1998.

Howell, K.C., B.T. Barden, M.W. Lo, "Application of Dynamical Systems Theory to Trajectory Design for a Libration Point Mission", JAS 45: 161 - 178, 1997.

Marchal, C., The Three-Body Problem, Elsevier, 1990.

Scheeres, D.J., D. Han, Y. Hou, "The Influence of Unstable Manifolds on Orbit Uncertainty," submitted to JGCD, 1999.